Nuclear Instruments and Methods in Physics Research A 338 (1994) 568–576
North-Holland

NUCLEAR
INSTRUMENTS
& METHODS
IN PHYSICS
RESEARCH
Section A

A γ-ray detection system for 3-D particle tracking in multiphase reactors

Faïçal Larachi [1], Gregory Kennedy [2], Jamal Chaouki *,[1]
École Polytechnique de Montréal, P.O. Box 6079, Station A, Montréal, Québec, Canada, H3C 3A7

(Received 16 August 1993)

A system employing eight NaI detectors has been developed for tracking particles moving in a three-phase fluidized bed reactor. One particle is tagged with typically 2 MBq of ^{46}Sc which emits high energy γ-rays. The system is calibrated by measuring the count-rates in the 8 detectors with the tagged particle placed at a number of locations in the reactor and then calculating the count-rates, using the Monte Carlo technique, at 19200 locations. In a tracking experiment, data are accumulated in the multiscaling mode and the coordinates of the moving particle are calculated by least-squares using the calibration map. With 30 ms counting intervals, the location of the particle is determined with a typical precision of 5 mm. The use of these data for determining velocity flow fields in multiphase reactors is illustrated.

1. Introduction

In chemical engineering research, the study of the hydrodynamics of multiphase reactors is relying increasingly on non-invasive techniques for the measurement of the flow fields. The development of these non-invasive techniques in fields such as nuclear medicine, physics and fluid mechanics research and the spectacular improvements in computer performance have both contributed to the increase in interest in the investigation of chemical reactor hydrodynamics. Among the most established applications of techniques based on ionizing radiation, one can cite X-ray transmission, and positron emission and neutron transmission tomography. These have been successfully utilized in voidage imaging of consolidated porous media, and granular or gas–liquid horizontal flows [1–3]. However, tomography usually provides information only on the flow morphology and not on the motion of the flowing phases. Recently, there has been a significant effort to develop γ-ray emission techniques for measuring positions and velocities in three dimensions in multiphase reactors. Flow field information has thus been obtained on the catalyst motion in gas–solid fluidized beds [4–6] and on the liquid motion in bubble columns [7–10].

The fluidized bed reactor used in this research contains solid particles maintained in suspension by upward flowing liquid and gas. One of the particles, the flow follower, is tagged with a γ-emitting radionuclide. The γ-rays are detected by an array of NaI scintillators. The count-rate in each detector depends on the distance to the particle and the amount of absorbing material in the reactor between particle and detector. The counts are recorded using multichannel scaling. Faster moving particles require shorter counting intervals. For each point in time, the position of the particle is calculated from the number of counts in all the detectors. This requires a mapping, for each detector, of count-rate as a function of position over the entire volume of the reactor. Since any change in density affects γ-ray absorption and thus the count-rates, the mapping must be redone for any change in reactor parameters.

The system developed in this research employs eight NaI detectors. The mapping is carried out by Monte Carlo calculation with parameters such as the γ-ray linear attenuation coefficient adjusted to fit count-rates measured at a number of calibration positions. For particle tracking, the flow follower positions are calculated using a least-squares approach. Tests have been conducted with gas–liquid–solid fluidization to assess the performance of the system as to its accuracy in determining flow follower positions and velocities.

[1] Department of Chemical Engineering.
[2] Energy Engineering Institute.
* Corresponding author.

SSDI 0168-9002(93)E0862-M

2. Experimental facility

Fig. 1 shows a schematic of the experimental facility built for the tracking experiments in a gas–liquid–solid reactor (FB) where 3 mm glass beads are fluidized. The reactor consists of a 100 mm diameter and 1500 mm high Plexiglas column fed in concurrent upflow by air and tap water at ambient temperature and atmospheric pressure. Liquid and gas circulation through the column are ensured respectively by a Moyno pump (Moyno 2L4, 24 GPM) and a gas compressor. After pressure reduction, the gas flows through a 20 μm sintered tube and disperses as small bubbles in the liquid stream. A three-stage distributor before the entrance region of the column ensures axisymmetrical flows in the reactor. In the distributor, the two-phase mixture traverses a 150 mm high cone packed with 4 mm glass beads, a sandwiched perforated plate and finally a 210 mm high bed packed with 2 mm glass beads. Two fine mesh screens located at each extremity of the column prevent the entrainment of the fluidized particles or their contact with the upper part of the distributor. Fluid throughputs, controlled by rotameters, and the solids inventory of the fluidized bed are set so as to maintain the three-phase emulsion level at 400 to 500 mm above the distributor. An overflow system on top of the column separates the gas from the liquid, the latter is circulated in closed loop to a thermostated 100 l buffer vessel while the former is vented to the atmosphere.

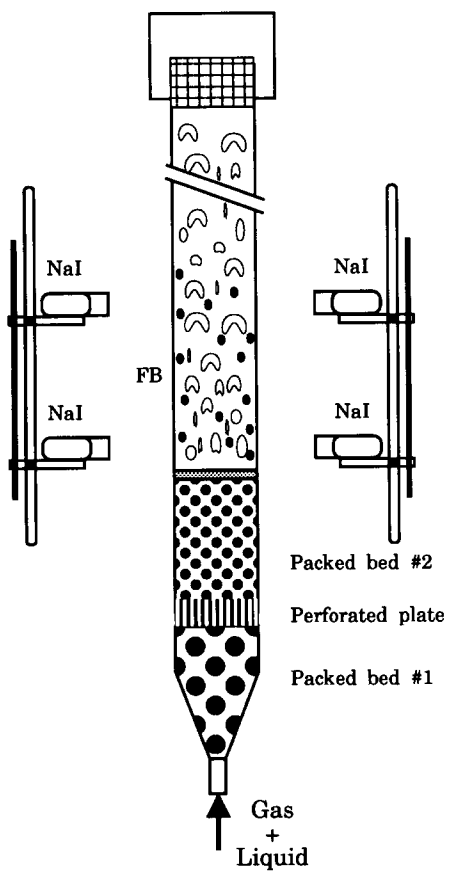

Fig. 1. Schematic of the experimental facility.

A number of aluminum probe ports along the column wall allow the insertion of Plexiglas rods used to place the tracer particle at the desired calibration positions. The rigid aluminum probe ports support the Plexiglas rods without vibration under actual flow conditions. Eight 76 mm by 76 mm NaI(Tl) scintillation detectors (Teledyne Isotopes model S-1212-I) are supported around the reactor on sliding rails. The configuration used for most of the measurements is shown in Fig. 1. The detectors are placed on two levels 110 mm and 370 mm above the bottom of the reactor. The four detectors on each level surround the reactor with 90° spacing. The distance between the front of the detector and the reactor wall is an important parameter. It determines the maximum count-rate when the tracer particle is close, as well as the rate of decrease in count-rate as the particle moves away. For most measurements, the detectors were 72 to 184 mm from the reactor.

2.1. Radioactive tracer

The tracer particle is made of a mixture of soda lime powder and scandium oxide melted at high temperature. With 10–12% Sc, the density of the 3 mm tracer particle is within 5% of that of the glass beads of the fluidized bed. The particle is coated with a diamond-like carbon layer, a few microns thick, deposited by a radiofrequency Ar–CH_4 plasma, in order to prevent its rupture due to attrition in the flow. The particle is activated in École Polytechnique's SLOWPOKE nuclear reactor. Neutron capture by ^{45}Sc produces ^{46}Sc which has a half-life of 83.8 d. Following beta decay, ^{46}Sc emits γ-rays of energies 889 and 1120 keV. In the calculations, these two γ-rays are modelled by two identical γ-rays with the average energy 1005 keV. The particle is not used until at least five days after activation in order to eliminate the shorter lived ^{24}Na activity. A tracer of the highest usable activity is produced in order to improve counting statistics. The NaI detectors saturate at about 10^5 counts/s. The activity produced is that which gives 90% of the saturation count-rate when the particle is near the reactor wall in front of the detector. For 72 mm detector–reactor distance, this activity is 1.85 MBq; for 184 mm distance it is 7.4 MBq.

2.2. Counting system

Each NaI(Tl) detector is connected to a non-NIM amplifier and bias supply workstation (EG&G ORTEC ACE Mate 925) which provides voltage distribution to the 10-stage PMT via a photomultiplier base (EG&G ORTEC PMB model 266) as well as signal amplification and discrimination (SCA mode). The discriminators are set to accept only pulses corresponding to full energy deposited in the detector. Thus, γ-rays which Compton scatter in the reactor are rejected. The logic pulses from the discriminators are sent to a personal computer which contains eight multichannel scaling boards (EG&G ORTEC ACE-MCS 4096 channels). Data are acquired simultaneously for the 8 detectors. When the MCS buffers are full (after 4096 counting intervals of typically 30 ms each), the acquisition is momentarily interrupted and the data are transferred and stored in binary format on PC RAM disks. It is retriggered after data transfer by a TTL signal sent in series to the input boards. After a tracking experiment, which lasts typically 6–12 hours, the acquired data are transferred to the PC hard disk and then converted to ASCII format before being sent via an RS-232 interface to a fast computer (IBM Risc 6000 A320H) where the tracer coordinates are reconstructed from the γ-ray counts.

3. Calculation of detector efficiency versus source location

In order to determine the position of the tagged particle from the number of counts in the 8 detectors, we need, for each detector, a map of counts as a function of the coordinates of the particle. Since a significant fraction of the γ-rays is absorbed by the material in the reactor, a new map is needed whenever the density of the emulsion changes. It is not feasible to construct the map by direct experimental measurements because of the large number of points which must be determined (several thousand). We have thus elected to model the reactor and the detectors and to calculate the detector efficiencies by the Monte Carlo method.

Theoretically, for a sampling period T, the number of recorded photopeak counts C can be expressed as follows [11]:

$$C = \frac{T\nu R\phi\epsilon}{1 + \tau\nu R\phi\epsilon}, \tag{1}$$

where R is the source activity and ν the number of γ-rays emitted per disintegration ($\nu = 2$ for ^{46}Sc). ϵ is the total detection efficiency; it is the probability that a γ-ray will emerge from the reactor without scattering and will interact with the detector. ϕ is the photopeak-to-total ratio of the detector. Thus $\phi\epsilon$ is the photopeak efficiency or the full energy peak efficiency. τ is the dead-time of the counting system per accepted pulse. In the above equation, the contribution of background counts to the dead-time is neglected. γ-rays which Compton scatter in the reactor are neglected because they do not contribute to the accepted (photopeak) counts. They do, however, contribute to the dead-time, but their omission from the denominator of Eq. (1) is justified by the fact that the dead-time correction is high only when the source is near the detector, which is where the unscattered γ-rays impinging on the detector far outnumber the scattered ones.

The exact calculation of the photopeak efficiency $\phi\epsilon$ for a point source contained in a cylindrical attenuating medium and situated, most often, off the axis of the detector is far from simple. Rigorous calculations of NaI(Tl) detector efficiencies for non-axial point sources in air using Monte Carlo procedures are available in many publications [12–16]. However, those dealing with a non-axial point source confined in a neutral attenuating material of defined geometry are rather scanty. A Monte Carlo procedure will be developed for the calculation of $\phi\epsilon$ in the case which is of interest to us.

Our measurements indicate that the peak-to-total ratio ϕ is fairly independent of the source–detector distance and of the angle between the source–detector line and the detector axis. We have thus adopted a constant value of 0.40 for ϕ for 1005 keV γ-rays. The factors that must be taken into account for the Monte Carlo calculation of the detection efficiency ϵ are:

i) The solid angle Ω subtended by the detector surface as seen from the tracer position.

ii) The probability of non-interaction f_a of γ-rays emitted within Ω with the material of the reactor. It is calculated as:

$$f_a(\alpha, \theta) = \exp(-\mu_R e(\alpha, \theta)), \tag{2}$$

where μ_R is the total linear attenuation coefficient of the fluidizing medium for 1005 keV γ-rays and $e(\alpha, \theta)$ is the path length travelled by the photons in the sampled direction determined by angles α and θ with respect to the detector. A geometrical construction for the determination of $e(\alpha, \theta)$ is depicted in Fig. 2 for a tracer situated off axis with photons entering from the lateral side of the crystal.

iii) The probability of interaction f_D of these γ-rays with the crystal. It is given by:

$$f_D(\alpha, \theta) = 1 - \exp(-\mu_D d(\alpha, \theta)), \tag{3}$$

where μ_D is the total linear attenuation coefficient (excluding coherent scattering) of the detector material and $d(\alpha, \theta)$ is the effective distance travelled in the crystal by an undisturbed γ-ray along the direction (α, θ), see also Fig. 2.

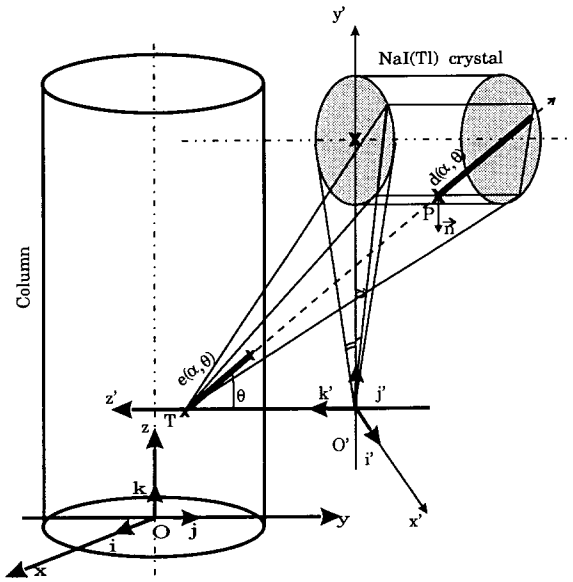

Fig. 2. Geometrical construction for the determination of the path length $e(\alpha, \theta)$ and the effective distance $d(\alpha, \theta)$ travelled by the photons in the reactor and the detector.

Finally, ϵ can be expressed as [17]:

$$\epsilon = \int\int_{\{\Omega\}} \frac{\boldsymbol{r}\cdot\boldsymbol{n}}{r^3} f_a(\alpha, \theta) f_D(\alpha, \theta)\, d\Sigma \qquad (4)$$

Here, $\boldsymbol{r}$ is the vector from point source T to a variable point P on the exposed surface of the crystal, $\boldsymbol{n}$ is an external unit vector locally normal to the surface at P and $d\Sigma$ is an infinitesimal area around P. Notice that the formula does not contain a correction factor for buildup since only unscattered photons are counted.

To estimate ϵ by Monte Carlo for a given position of the tracer in the reactor, the surface integral of Eq. (4) is evaluated by sampling at random several thousand directions (α, θ). We have found that the improvement in precision with 4000 directions compared to 1000 is insignificant. Thus, all the calculations are performed with 1000 directions. It was possible to achieve sufficient precision with only 1000 directions because only directions in the vicinity of the detector are sampled [16]. An appropriate statistical weight $\omega(\alpha, \theta)$ is assigned to each sampled direction (α, θ). With the hypothesis of isotropic emission, angles α and θ are sampled independently [16,18] so that $\omega(\alpha, \theta) = \zeta(\alpha)\zeta(\theta)$. Evaluation of these weights is discussed by Beam et al. [16]. Routines for congruential random number generators of rectangular distributions have been taken from Press et al. [19]. Conjointly, for each sampled direction (α, θ), probabilities $f_D(\alpha, \theta)$ and $f_a(\alpha, \theta)$ must be determined. Finally, the averaged value of the product $\zeta(\alpha)\zeta(\theta)f_D(\alpha, \theta)f_a(\alpha, \theta)$ for all sampled directions constitutes an unbiased estimator of the total efficiency:

$$\epsilon = \frac{1}{N}\sum_{1}^{N} \zeta(\alpha)\zeta(\theta) f_D(\alpha, \theta) f_a(\alpha, \theta). \qquad (5)$$

For the calculation of the effective distance $d(\alpha, \theta)$ in the detector, the points where the γ-ray enters and leaves the detector must be determined. It may enter through the front or the side and may leave through the back or the side. This calculation is carried out in the particle–detector frame $(O', \boldsymbol{i}', \boldsymbol{j}', \boldsymbol{k}')$ and the associated weighting factors are based on the work of Beam et al. [16]. The path length $e(\alpha, \theta)$ which the γ-ray must travel in the reactor without being scattered is determined by calculating the intersection of a line and a right cylinder in the reactor frame $(O, \boldsymbol{i}, \boldsymbol{j}, \boldsymbol{k})$. To achieve this, transformation formulae were developed to switch from the particle-detector coordinate frame $(O', \boldsymbol{i}', \boldsymbol{j}', \boldsymbol{k}')$ to the reactor coordinate frame $(O, \boldsymbol{i}, \boldsymbol{j}, \boldsymbol{k})$.

The Monte Carlo calculations are verified by comparing the calculated counts for the 8 detectors with those measured by placing the radioactive particle at a number of locations in the reactor. These calibrations permit the verification of the values used for the source activity and the dead-time and the adjustment of the value used for the linear attenuation coefficient of the reactor emulsion.

For each detector, the Monte Carlo calculation is performed for 19200 locations in the reactor: for 60 values of axial coordinate z, 8 radii and 40 azimuthal angles. With 8 detectors and 1000 directions (α, θ) calculated for each of the 19200 locations, the total of 1.54×10^8 calculations requires 30 cpu hours on an IBM Risc 6000 A320H computer in single precision mode.

4. Calculation of the tracer particle coordinates from the γ-ray counts

Once the map has been constructed, it is used to determine tracer particle positions for runs which may last several hours. With a typical counting interval of 30 ms, this implies the determination of several hundred thousand positions. The counts in each 30 ms interval vary typically from 10 to 1000 and are of course subject to statistical fluctuations which will limit the precision of the coordinates which are determined. A given number of counts in one detector implies that the particle is located on an isocount sphere. Actually, the sphere is distorted by the anisotropicity of the detector and by the attenuation of the emulsion in the reactor. The counts from several detectors imply that the particle is located at the intersection of the corre-

sponding distorted spheres. Because of the statistical imprecision in the counts, these isocount surfaces are imprecise and a strategy must be adopted to calculate the optimal intersection point. A least-squares approach has been adopted. The 8 measured counts are compared with the Monte Carlo calculations at each of the 19 200 grid points. The point is found which minimizes χ^2:

$$\chi^2 = \sum_{i=1}^{8} \frac{(C_i - M_i)^2}{\sigma_i^2}, \tag{6}$$

where C_i is the calculated count for detector i, M_i is the measured count and θ_i is the statistical uncertainty (the square-root of C_i).

Even with 19 200 grid points, the coordinates of the best grid point are not of sufficient accuracy for particle tracking. Hence, the search is continued in the neighbourhood of this grid point. The coordinates r, θ and z are varied in a search for the point whose calculated counts minimize χ^2. It is not necessary to perform a Monte Carlo calculation for each new point tested because, for small variations in position, no accuracy is lost if it is assumed that the detector efficiency varies as the inverse square of the distance between the source and the center of the detector. Thus the count at the new location is calculated from C, the count at the best grid point, using the following equation:

$$C^* = \frac{TC\left(\frac{r}{r^*}\right)^2 \exp(\mu_R(e-e^*))}{T - \tau C + \tau\left(\frac{r}{r^*}\right)^2 C \exp(\mu_R(e-e^*))}. \tag{7}$$

Here the symbols with asterisks refer to the new location and the others to the nearby grid point, r is the distance between the source and the geometric center of the detector and e is the path length traversed by the γ-ray through the emulsion along r.

For each of the 4096 time intervals other than the first in each packet of data, the search is carried out over the 1000 grid points closest to the previous best grid point, rather than all 19 200, because the particle cannot move very far over one time interval. With this elimination of wasted calculation time, the average cpu time needed to determine one tracer position is 0.3 s. Thus, for a typical tracking experiment lasting 8 h, the calculation of one million tracer particle locations requires 80 cpu hours.

5. Results and discussion

The calculated efficiencies were verified at 150 points inside the reactor by inserting the radioactive source, on the end of a Plexiglas rod, to 5 horizontal locations through 30 ports in the column wall. At each point, the γ-rays were counted for 7.5 s in order to achieve good counting statistics in each of the 8 detectors. The comparison between the calculated counts and the measurements depends on the values used in the calculations for the source activity R, the dead-time τ and the attenuation coefficient of the three-phase emulsion, μ_R. In fact, for each detector, the optimum values for these three parameters are found by minimizing the following objective function:

$$\Phi^2 = \sum_{i=1}^{150} \left(\frac{C_i - M_i}{C_i + M_i}\right)^2, \tag{8}$$

where the C_i are the calculated counts and M_i the measured counts. Table 1 shows the parameters obtained for each detector in the case of a 10 MBq source in a fluidized bed of air, water and glass beads and the detectors 220 mm from the column. The parameters are consistent from one detector to another. Part of the variation in μ_R may be due to variations in density in different regions of the reactor and part of the variation in R may in fact be due to slightly

Table 1
Dead-time τ, emulsion linear attenuation coefficient μ_R and source activity R obtained by optimizing the Monte Carlo calculation of Eqs. (1) and (2) to agree with the measured counts. Sampling period = 7.5 s, source strength = 10 MBq

Detector no.	τ [μs]	μ_R [m^{-1}]	R [MBq]
1	2.4	6.3	10.6
2	2.7	7.1	9.5
3	2.5	6.5	10.3
4	2.6	7.0	9.6
5	2.7	7.2	9.3
6	2.4	6.4	10.5
7	2.4	6.5	10.4
8	2.6	6.8	9.8

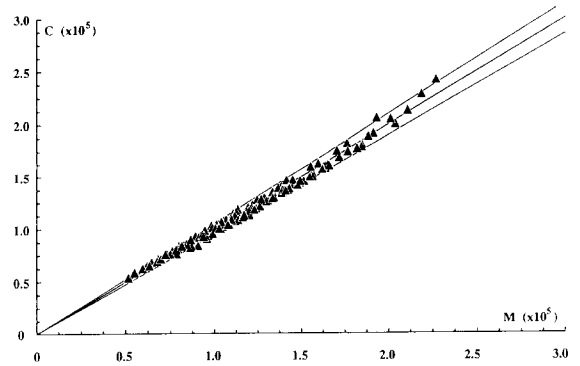

Fig. 3. Parity plot of the calculated and measured counts for detector no. 7. Sampling period = 7.5 s, source strength = 10 MBq.

different discriminator settings among the detectors. The parameters obtained in this manner are used for the calculations of the counts at the 19 200 grid points. A parity plot of the measured counts and those calculated by the model is shown in Fig. 3 for detector no. 7. The +5% and −5% limits are also shown. The agreement between measured and calculated counts is also satisfactory for the other detectors. The calibration

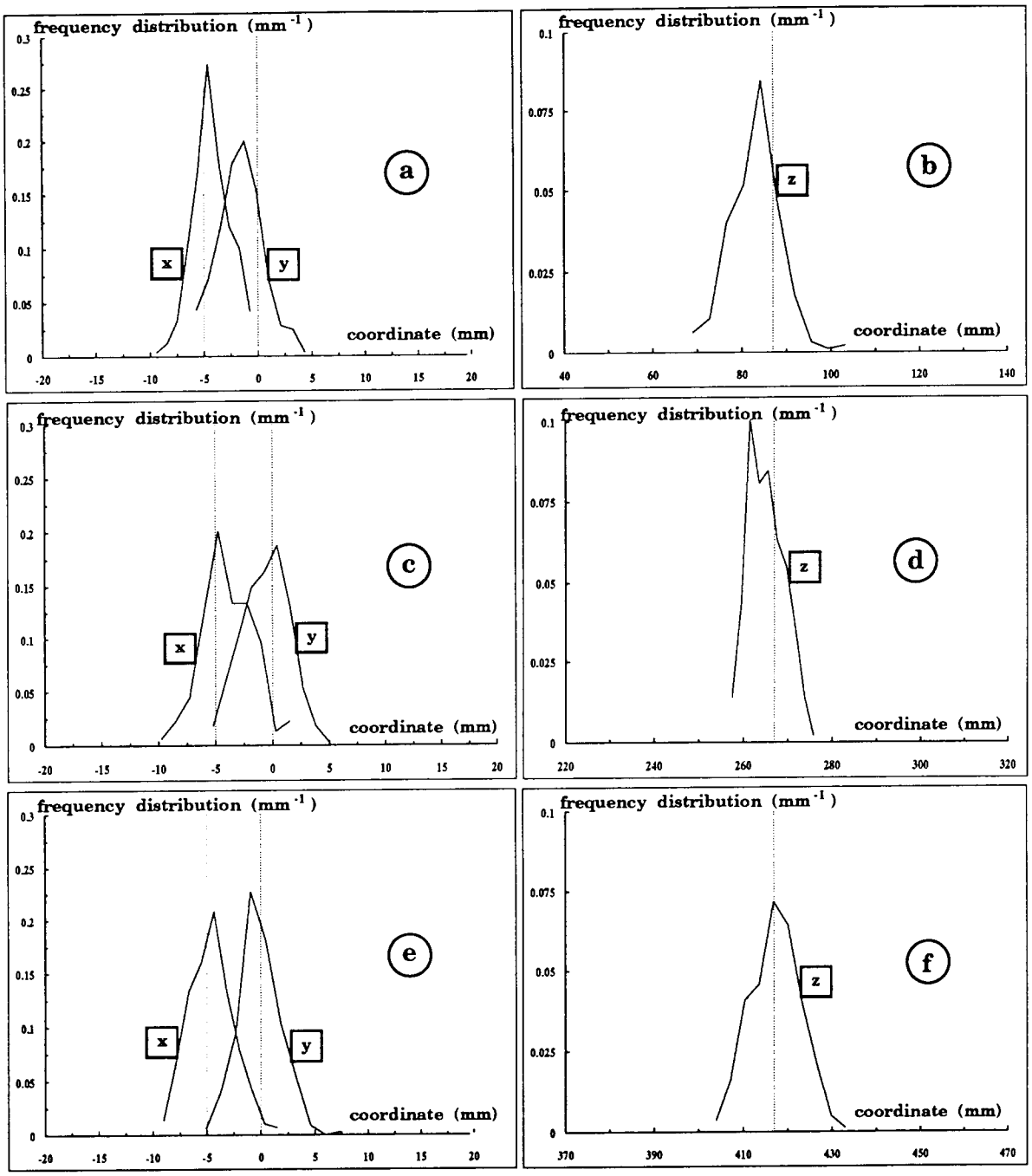

Fig. 4. Frequency distributions of the coordinates x, y and z determined at: $x = -5$, $y = 0$, $z = 87$ (a)–(b); $x = -5$, $y = 0$, $z = 267$ mm (c)–(d) and $x = -5$, $y = 0$, $z = 417$ mm (e)–(f). Sampling period = 30 ms, source strength = 1.85 MBq.

procedure described here is repeated for every run since the density of the emulsion changes with fluid velocities.

The accuracy and precision of the system have been evaluated for determining the position of a stationary and a moving particle. Fig. 4 shows the frequency distributions of the coordinates (x, y, z) determined for a particle positioned at three levels in the three-phase emulsion: $z = 87$ mm above the distributor near the bottom level detectors, $z = 267$ mm, and $z = 417$ mm near the top level detectors. The detectors were 72 mm from the wall of the reactor. At each position, data were collected for 250 counting intervals of 30 ms (33 Hz). The vertical dashed lines indicate the true geometrical coordinates where the tracer was maintained. It may be seen that horizontal coordinate distributions look similar with comparable standard deviations regardless of position. On the contrary, the axial coordinate frequency distributions are very sensitive to axial location. They are narrower for positions between the detector levels. At the levels where 4 detectors are located, the axial coordinate frequency distributions are broader because these 4 detectors are insensitive to variations in the z coordinate. In all cases, the 3-D standard deviation $\sigma = (\sigma_x^2 + \sigma_y^2 + \sigma_z^2)^{1/2}$ is dominated by the axial standard deviation σ_z, which is typically 5 mm. This resolution is adequate for tracking experiments. In the light of these results, we feel that it may be possible to obtain a slight improvement in σ_z by placing the detectors on four levels of two rather than on two levels of four.

Fig. 5 shows the 3-D cross-sectional averaged standard deviations as a function of the axial coordinate for all the 150 calibration points with the detectors 72 mm from the column wall and a sampling frequency of 33 Hz. Data obtained at 33 Hz with the detectors 184 mm from the column wall and a radioactive source 4 times stronger (7.4 MBq) are also shown in Fig. 5. Horizontal coordinates are always determined with better precision than the axial coordinate. At 33 Hz, σ_x and σ_y vary between 1 and 2 mm while σ_z varies between 3 and 8 mm. These intervals are represented on the figure by the vertical bars on the measured 3-D averaged standard deviations. Theoretical axial standard deviations $C^{1/2}/(\partial C/\partial z)_{x=y=0}$ as predicted from Monte Carlo calculations along the reactor axis are also shown for 2 detectors from the lower level and 2 from the upper level for the detectors 72 mm from the column. The loss of sensitivity when the tracer is near the level of the detector is very well illustrated by the figure. The advantage of multiple detectors is also clearly shown with the 3-D standard deviations obtained using 8 detectors lying well below the σ_z of any individual detector. Fig. 5 also illustrates that the spatial resolutions with the detectors 72 mm from the

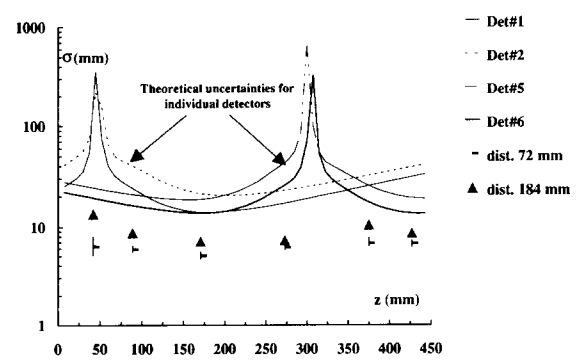

Fig. 5. Influence of the distance of the detectors from the column wall on the 3-D cross-sectionally averaged standard deviations. Comparison with the theoretical axial standard deviation σ_z calculated along the reactor axis for individual detectors. Sampling period = 30 ms, source strengths = 1.85 and 7.4 MBq.

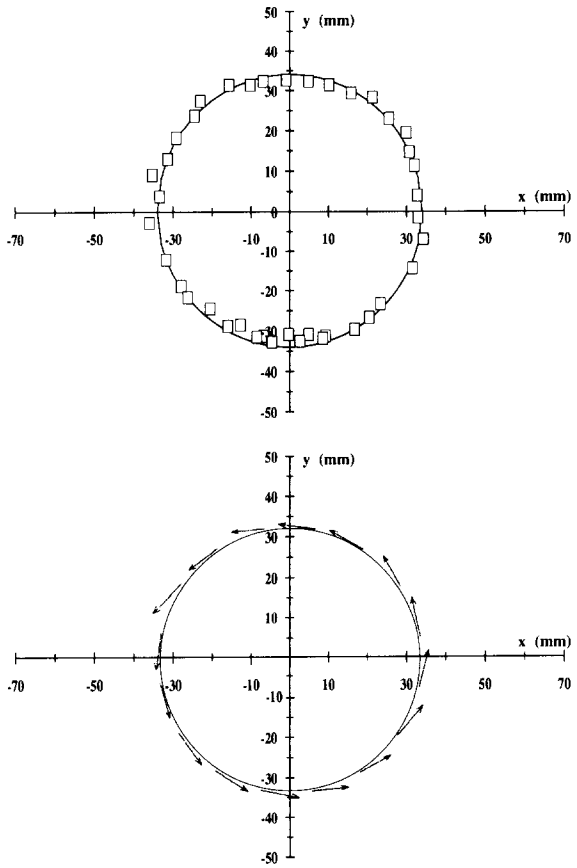

Fig. 6. (a) Horizontal positions determined for one orbit of the particle with detectors 72 mm from the wall. (b) The corresponding horizontal velocities averaged over 120 s. Sampling period = 240 ms, source strength = 1.85 MBq.

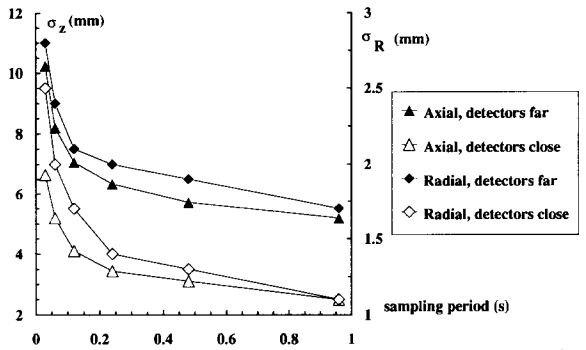

Fig. 7. Influence of the detector position and sampling period on the standard deviations σ_R and σ_z for a circular trajectory. Source strengths = 1.85 and 7.4 MBq.

reactor are always better than those obtained with the detectors 184 mm away.

The performance of the system for a particle moving in a circular trajectory was evaluated by attaching it to the end of a Plexiglas rod projecting horizontally from an aluminum rod maintained on the vertical axis of the reactor by a ball-bearing. The aluminum rod was motor driven and made one rotation every 9 s. The particle revolved in a horizontal circle of radius 34 mm at a height $z = 373$ mm. Measurements were carried out with the detectors at 72 mm and at 184 mm from the column wall. In each case, counts were acquired in the 8 detectors for 120 s with sampling intervals of 0.03, 0.06, 0.12, 0.24, 0.48 and 0.96 s. Fig. 6 shows the horizontal positions determined for one orbit of the particle with the detectors 72 mm from the column and a sampling interval of 0.24 s. The horizontal components of the velocities are shown in the lower part of the figure. They were calculated by subtracting the coordinates of successive positions and dividing by the counting interval. The vectors shown are the averages over the 120 s measurement period, for 16 regions along the circle. The average axial and radial velocity components were found to be approximately zero and the average azimuthal velocity was found to be the expected value of 24 mm/s.

Fig. 7 shows the influence of the detector positions and of the sampling period on the standard deviations σ_R and σ_z of the radius and height of the reconstructed trajectories. As Fig. 5 showed for static sources, spatial resolutions are always better with the detectors closer to the column wall. The decrease of σ_R and σ_z with sampling period is monotonic but sharper for short sampling periods. For the 0.03 s sampling period, σ_R and σ_z compare very well with those obtained at the same height with stationary sources.

6. Application to solid flow field measurements in multiphase reactors

As an illustration of the performance of the system in a real situation, Figs. 8 and 9 show results obtained with the detectors 72 mm from the column and the 1.85 MBq tagged particle moving in a three-phase fluidized bed of 3 mm glass beads fluidized by air and water with superficial velocities of 25 mm/s and 60 mm/s respectively. Over 8×10^5 data/detector were acquired at 33 Hz during 6.8 h. Fig. 8 shows the movement in the axial direction over the first 60 s of the measurement (roughly 2000 reconstructed locations) and shows two types of motion of the tracer: random jumps superimposed on slowly varying cycles extending from the top of the bed to the distributor. Since the flow is axisymmetrical, it suffices to plot the calculated mean Eulerian velocity field of the solid particles in a 2-D r–z frame as Fig. 9 illustrates. Each velocity vector shown is the average of all the velocities determined at a given location. Details on velocity calculations can be found in ref. [7]. Flow diagnosis and analysis of other hydrodynamic quantities that can be obtained with this technique can lead to a much more profound understanding of the phenomena involved in the motion of discrete particles in multiphase reactors than could be obtained using any previously available techniques.

7. Conclusion

A non-invasive 3-D position sensitive γ-ray emission technique has been developed and applied to investigate the discrete solid-phase motion in three-phase fluidized beds. A methodology and an algorithm for tracer coordinate rendition from the γ-counts provided by an array of strategically positioned scintillation de-

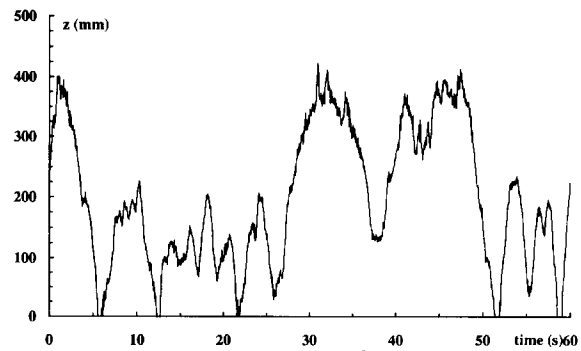

Fig. 8. Tracking of labelled tracer particle in a three-phase fluidized bed: variation with time of axial component. Sampling period = 30 ms, source strength = 1.85 MBq.

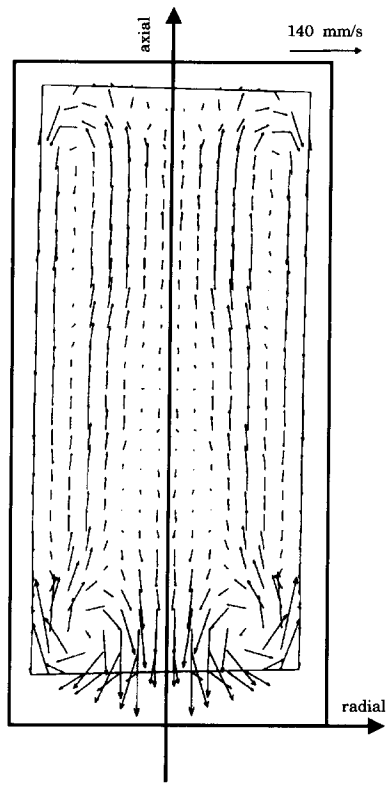

Fig. 9. Mean Eulerian velocity field of the axisymmetrical solids flow in a three-phase fluidized bed versus location in the $r-z$ frame. The length of each arrow is proportional to the average velocity in the $r-z$ plane at this position and the arrowheads indicate the direction of flow. Sampling period = 30 ms, source strength = 1.85 MBq.

tectors, have also been developed and their performance detailed.

With a 0.03 s counting interval, horizontal coordinates of the tracer particle can be determined with a precision better than 2 mm. In the axial direction, the precision is typically 5 mm and it varies with axial position. For the solids velocities encountered, the achieved precision is adequate for determining velocity fields in three-phase fluidized beds.

Acknowledgements

The authors gratefully acknowledge financial support from the Natural Sciences and Engineering Research Council of Canada. Thanks are also addressed to Dr. M. Cassanello for her unselfish help in the execution of many of the calculations.

References

[1] M.E. Hosseini-Ashrafi and U. Tüzün Chem. Eng. Sci. 48 (1993) 53.
[2] J.K. Jasti and H.S. Fogler, AIChE J. 38 (1992) 481.
[3] V. Modi, C. Gnafakis and C.C. Gryte, Chem. Eng. Commun. 116 (1992) 117.
[4] D. Moslemian, M.M. Chen and B.T. Chao, Part. Sci. Technol. 7 (1989) 335.
[5] N. Devanathan and D. Moslemian, Symp. Small Comp. Fluid Mech., ASME Winter Annual Meeting, Chicago, Illinois (1988) 53.
[6] J.S. Lin, M.M. Chen and B.T. Chao, AIChE J. 31 (1985) 465.
[7] M.P. Dudukovic, N. Devanathan and R. Holub, Rev. Inst. Franc. Pétr. 46 (1991) 439.
[8] Y.B. Yang, N. Devanathan and M.P. Dudukovic, Chem. Eng. Sci. 47 (1992) 2859.
[9] Y.B. Yang, N. Devanathan and M.P. Dudukovic, AIChE Annual Meeting, November 1–6, Miami Beach Florida, USA (1992).
[10] N. Devanathan, D. Moslemian and M.P. Dudukovic, Chem. Eng. Sci. 45 (1990) 2285.
[11] N. Tsoulfanidis, Measurement and Detection of Radiation, Series in Nuclear Engineering (McGraw-Hill, 1983).
[12] S.N. Kaplanis, Int. J. Appl. Radiat. Isot. 29 (1978) 543.
[13] S.N. Kaplanis, Nucl. Instr. and Meth. 188 (1981) 353.
[14] J.I. Trombka, Nucl. Instr. and Meth. 93 (1971) 119.
[15] J. Lippert, Int. J.. Appl. Radiat. Isot. 34 (1983) 1097.
[16] G.B. Beam, L. Wielopolski, R.P. Gardner and K. Verghese, Nucl. Instr. and Meth. 154 (1978) 501.
[17] L. Moens, J. De Donder, X.L. Lin, F. De Corte, A. De Wispelaere, A. Simonits and J. Hoste, Nucl. Instr. and Meth. 187 (1981) 451.
[18] S.N. Kaplanis, Int. J. Appl. Radiat. Isot. 33 (1982) 127.
[19] W.H. Press, B.P. Flannery, S.A. Teukolsky and W.T. Vetterling, Numerical Recipes. The Art of Scientific Computing – Fortran Version – (Cambridge University Press, USA, 1989).